Analytica Chimica Acta 1156 (2021) 338206

Contents lists available at ScienceDirect

Analytica Chimica Acta

journal homepage: www.elsevier.com/locate/aca

Tutorial

A down-to-earth analyst view of rotational ambiguity in second-order calibration with multivariate curve resolution – a tutorial

Alejandro C. Olivieri

Departamento de Química Analítica, Facultad de Ciencias Bioquímicas y Farmacéuticas, Universidad Nacional de Rosario, Instituto de Química Rosario (CONICET-UNR), Suipacha 531 (2000), Rosario, Argentina

HIGHLIGHTS

- Rotational ambiguity is ubiquitous in multivariate curve resolution.
- The phenomenon is explained in simple terms.
- Simulated and experimental data are described.
- The potential impact on prediction uncertainty is underlined.

GRAPHICAL ABSTRACT

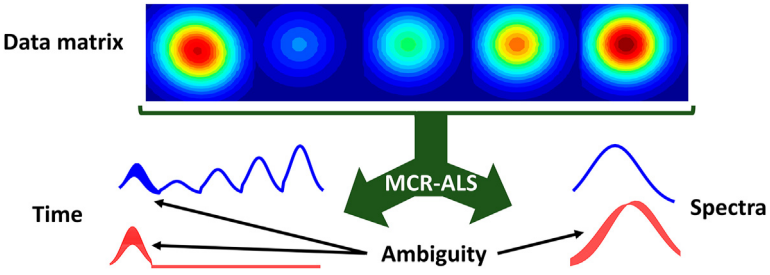

ARTICLE INFO

Article history:
Received 29 October 2020
Received in revised form
6 January 2021
Accepted 7 January 2021
Available online 18 January 2021

Keywords:
Multivariate curve resolution
Alternating least-squares
Rotational ambiguity
Concentration uncertainty

ABSTRACT

Rotational ambiguity is a phenomenon with the potential of generating an uncertainty in the estimation of analyte concentrations in protocols based on matrix instrumental data processed by multivariate curve resolution - alternating least-squares (MCR-ALS). This is particularly relevant when the second-order advantage is to be achieved, i.e., when selected analytes are determined in unknown samples having unexpected constituents, not considered in the calibration set of samples. It is therefore imperative that analytical chemists developing second-order multivariate calibration methods using MCR-ALS acknowledge the relevance of this issue, and more importantly, have access to the required tools to size the relative impact of this potential source of uncertainty on the estimated analyte concentrations. The purpose of this tutorial is to provide a down-to-earth view of rotational ambiguity, by studying in detail a synthetic example mimicking a typical chromatographic-spectral experiment, where a set of calibration samples is joined with an unknown sample having an uncalibrated interference. After explaining the background information needed to understand the origin of the phenomenon, the available tools for the estimation of the feasible MCR-ALS solutions and the derived uncertainty on analyte predictions will be discussed. A multi-component experimental system will also be discussed, stressing the fact that rotational ambiguity uncertainties, however small, should always be estimated and reported.

E-mail address: olivieri@iquir-conicet.gov.ar.

https://doi.org/10.1016/j.aca.2021.338206
0003-2670/

Contents

1. Introduction

Multivariate curve resolution by alternating least-squares (MCR-ALS) is a widely employed model in different research areas for processing data from various sources [1–3]. The underlying strategy is powerful enough to allow one for the description, identification and quantitation of the sample constituents, when they cannot be easily isolated, when the samples are too complex and/or when the studied chemical processes are partially or even completely unknown. The basic idea behind MCR-ALS is that a data table or matrix can be decomposed into the product of two smaller matrices by resorting to a bilinear model, and that this can be accomplished with a limited information, or even none, regarding the system under scrutiny. It is common to collect in one of the two smaller matrices the composition information on the system, in terms of number of components and their relative concentrations. The remaining small matrix collects information on the instrumental signals for the pure components.

A particularly useful MCR-ALS variant is the extended one [4,5], which has been applied to second-order analytical data, mainly for developing quantitative multivariate calibration protocols for analytes in complex samples [6]. This model is often able to achieve the important second-order advantage [7], which can be defined as the ability to quantitate calibrated analytes in the presence of uncalibrated (also called unexpected) sample components.

A potential source of uncertainty in the MCR-ALS decomposition results is the so-called rotational ambiguity [8,9]. Despite the fact that this subject is known from ca. fifty years ago [10], and that many advances have been made regarding the estimation of the extent of rotational ambiguity in bilinear decompositions [11–14], the issue is almost absent in analytically oriented experimental reports. In particular, a research line was initiated in the author's laboratory on second-order calibration about thirty years ago, although the potential problems associated with rotational ambiguity were not appreciated until recently. After discussions with experts in the field during the meeting Topics in Chemometrics (TIC) held in 2017 in Newcastle, Australia, it was clear that the subject deserved to be studied, understood and considered as a potential source of uncertainty in our calibration protocols.

The absence of the estimation of rotational ambiguity in experimental second-order MCR-ALS calibration procedures may be due to the fact that part of the theory behind the phenomenon has been developed using abstract projections in principal component space [8–14]. Many reports have been published in specialized chemometric journals, which are not usually read by analytical chemists, even those using chemometrics for assisting the development of new analytical protocols. Therefore, the main purpose of the present tutorial is to call the attention of analytical chemists on the subject, and to describe the available tools to estimate the relative impact of this important phenomenon in the estimation of analyte concentrations with second-order multivariate calibration.

The tutorial is organized as follows: first a brief discussion on MCR-ALS is presented, then a simple two-component synthetic example is discussed to aid in understanding the basics behind rotational ambiguity, followed by a description of the uncertainties that may affect the analyte estimation and the tools available for its calculation. Although two-component systems may be too simple from the point of view of advanced theoretical studies, the former are still useful to illustrate the basic notions behind rotational ambiguity. An experimental data set will also be discussed, including the estimated relative impact of rotational ambiguity on the predicted analyte concentrations. The final section is devoted to recent work on the effect produced by the phenomenon in some special cases of second-order data whose research is under way.

2. A brief description of MCR-ALS

From a mathematical point of view, MCR-ALS designates an algorithm for solving the bilinear decomposition of a data matrix **D** in the product of two matrices [1]:

$$\mathbf{D} = \mathbf{C}\,\mathbf{S}^{\mathrm{T}} + \mathbf{E} \tag{1}$$

where **C** and **S** are the two matrices to be obtained after decomposition (the superscript 'T' stands for matrix transposition), and **E** is a matrix containing the error contributions which have to be minimized by the algorithm. In chemical studies, it is usual to employ the letters **C** and **S** to denote concentration and spectral data respectively, although the implications of the bilinear decomposition are more general. More details on the MCR-ALS operation and applications can be found in the specific literature [1–6].

From equation (1), a generic element of **D**, named $d(i,j)$ (i and j

are the row and column indexes for a specific matrix element respectively) can be written as (errors not considered):

$$d(i,j) = \sum_{n=1}^{N} c(i,n)\ \ s(j,n) \qquad (2)$$

where the index n identifies a given sample component, and N the total number of components. It is customary to collect all c (i,n) values into a vector $\mathbf{c}_n$, which is a column of **C**, and all s (j,n) values into a vector $\mathbf{s}_n$, which is a column of **S**. Thus **C** and **S** are of size (I,N) and (J,N), where I and J are the number of measured channels in each instrumental mode. These matrix sizes demand the transposition of **S** in equation (1) for consistency.

Equation (1) expresses two commonly obeyed laws in mixture analysis: (1) additivity of the signals, since the overall signal is given by the sum of the contributing signals from the sample constituents, hence the summation over the number of components, and (2) linearity, meaning that the signal from each constituent is directly proportional to it is concentration (Lambert-Beer law in absorption spectroscopy or its analogues in other instrumental measurements), thus the signal for each component is proportional to c (i,n), and the proportionality coefficient is s (j,n).

In analytical second-order calibration using MCR-ALS, the usual procedure involves the preparation of calibration standards, followed by measurement of matrix signals for each calibration and future test samples. The matrix for each test sample is joined with those for the calibration samples to build an augmented matrix $\mathbf{D}_{aug}$, by placing all the participating matrices side by side along the elution time direction. The reasons for applying this procedure can be found in specific reports [15–17].

If both signal additivity and the linear law hold, the augmented data matrix can be subjected to decomposition according to a model analogous to (1) into the product of the matrix of augmented time profiles $\mathbf{C}_{aug}$ and the matrix of spectral profiles **S** (the error term **E** is dropped for simplicity):

$$\mathbf{D}_{aug} = \mathbf{C}_{aug}\ \mathbf{S}^{T} \qquad (3)$$

The matrix $\mathbf{C}_{aug}$ contains successive sub-profiles of all components for all samples, in the same order which was employed to build $\mathbf{D}_{aug}$. Once the analyte of interest is selected from the N sample components, each sub-profile of $\mathbf{C}_{aug}$ is integrated, and the areas for the analyte in the calibration samples are used to build a linear calibration graph. Finally, the area of the analyte sub-profile in the test sample is interpolated in the latter graph, allowing one to estimate the analyte concentration [15].

3. Ambiguities in bilinear decomposition

As the Oxford Dictionary dictates, ambiguity is the quality of being open to more than one interpretation. In this sense, there are different types of ambiguities in finding $\mathbf{C}_{aug}$ and **S** when performing the decomposition of $\mathbf{D}_{aug}$. One of them is the component permutation ambiguity, which is related to the fact that the order of the columns of $\mathbf{C}_{aug}$ and **S** are arbitrary and can be permuted without changing $\mathbf{D}_{aug}$. This ambiguity is not serious, because one can identify the analyte of interest among the various sample components, independently on the order of component indexes, by comparison of the spectral profiles (the columns of **S**) with the known pure analyte spectrum. However, it may become an issue when developing automatic procedures for the identification of specific components.

Another ambiguity is related to the scale. It is easy to see in equation (3) that by multiplying any column of $\mathbf{C}_{aug}$ by a number, and dividing the associated column of **S** by the same number, the product of ($\mathbf{C}_{aug}\ \mathbf{S}^{T}$) is unchanged. This ambiguity is usually solved by fixing the scale of **S** during decomposition. The most common procedure involves forcing each column of **S** to have a unit 2-norm, which means that the squared root of the sum of the squared elements of each column of **S** is forced to be 1. With this strategy, varying component concentrations will be reflected only in the areas of the sub-profiles of $\mathbf{C}_{aug}$.

The third type of ambiguity is the rotational one, and refers to the existence of more than one solution for the bilinear decomposition, beyond permutation and scaling issues. Given that this may affect the analytical performance of an MCR-ALS protocol developed with matrix data, it is imperative to understand the phenomenon, and more importantly, to estimate its effect on predicted analyte concentrations. The remainder of the present report is devoted to this important issue and its consequences for second-order multivariate calibration protocols.

4. A synthetic example

To illustrate the matter in an analytical context, a simple mixture problem is chosen, having two constituents: one of them is the analyte of interest and the other one an interferent. The analyte

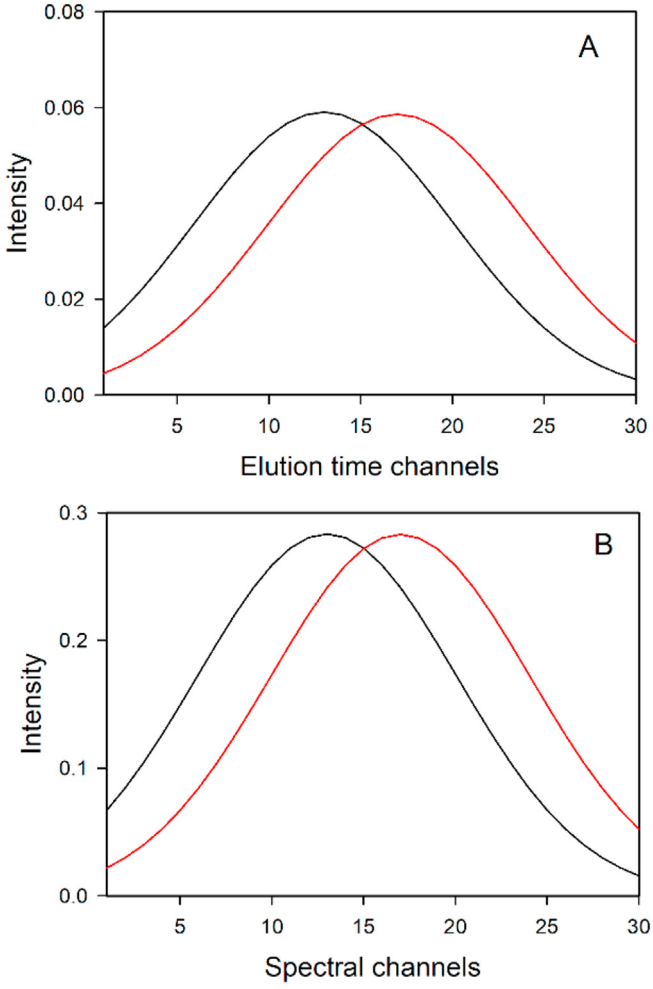

Fig. 1. A) Pure chromatographic profiles of two sample components in the elution time mode. B) Pure spectral profiles for the same components. Black lines, analyte of interest, red lines, interferent. (For interpretation of the references to colour in this figure legend, the reader is referred to the Web version of this article.)

is present in pure form in four calibration samples, with concentrations given by 0.25, 0.5, 0.75 and 1 arbitrary units. One test sample is analyzed, having both the analyte and the interferent at 0.5 concentration units. This mimics the typical case where the second-order advantage is to be achieved, to be able to quantitate the analyte in the test sample even in the presence of an uncalibrated interferent.

In this artificially prepared case, the properties of both constituents are known in pure form in both instrumental modes, which are taken as the elution time and the spectral mode, mimicking a chromatographic experiment with spectral detection (Fig. 1). The constituent profiles are seriously overlapped in both modes, so that univariate calibration is not a viable protocol for analyte determination. The ideal augmented profiles in the time mode for both constituents are shown in Fig. 2. Notice that the augmented profiles have five sub-profiles each, one corresponding to the test sample, and four to each of the calibration samples.

Once the samples are "prepared" with the analyte and interferent concentrations discussed above, the data are measured, resulting in five data matrices. In the present case, "prepared" means "computer generated", whereas in an experimental case it would mean "produced in the laboratory". The measurements involve 30 channels in the time mode and 30 wavelengths in the spectral mode, hence each matrix is of size 30 × 30 data points. Contour plots for the data matrices are shown in Fig. 3, for the test sample and for the four calibration samples. They are placed side by side along the time direction, building the augmented data matrix $\mathbf{D}_{aug}$ which will then be submitted to MCR-ALS bilinear decomposition (Fig. 3). The pertinent question is: will MCR-ALS retrieve the same $\mathbf{C}_{aug}$ and $\mathbf{S}$ profiles used to "prepare" the samples, i.e., the correct pure component profiles? The answer to this question is the key to understand the phenomenon of rotational ambiguity, as will be clear below.

5. The meaning of rotational ambiguity in MCR-ALS

Without requiring any special conditions to the bilinear decomposition, there are infinite pairs of $\mathbf{C}_{aug}$ and $\mathbf{S}$ matrices satisfying equation (3). One way of limiting the solutions is to enforce $\mathbf{C}_{aug}$ and $\mathbf{S}$ to fulfil certain properties, which are known as

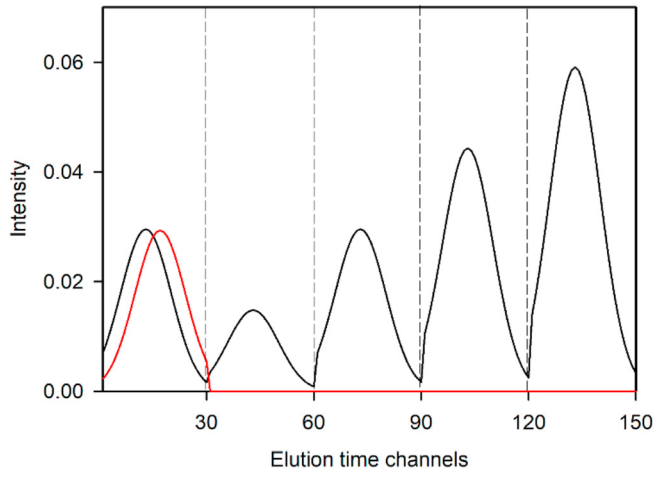

Fig. 2. Augmented time profiles for the two sample components. Black line, analyte of interest, red line, interferent. The vertical dashed lines separate the sub-profiles for each sample. The first sub-profiles on the left corresponds to the test sample, while three subsequent ones correspond to the four calibration samples, in the order of increasing analyte concentration. (For interpretation of the references to colour in this figure legend, the reader is referred to the Web version of this article.)

constraints. The constraints follow chemically sensible principles, such as: (1) non-negativity, for constituent concentrations and for spectral signals which may be positive or zero, (2) correspondence between species and samples in experiments where some constituents are absent in certain samples, (3) unimodality, for evolving chromatographic or kinetic signals showing a single maximum, (4) selectivity, for regions in any of the data modes where the signal from a single constituent is known to exist, (5) local rank, for windows in any of the data modes where the signals from some sample constituents are known to be absent, (6) known values, when the analyst knows from previous spectral or concentration information their values in certain channels, (7) area correlation constraint, which performs a linear regression of the areas under the sub-profiles for the analyte against its nominal concentrations in the calibration set of samples, (8) trilinearity, when the shapes of the profiles in both instrumental modes are constant in all samples, etc. See refs. [18–30] for details on the meaning and application of the latter and other constraints. Finally, to avoid scaling problems during decomposition, either normalization of spectra or closure conditions are applied. The latter are due to the fulfilment of a mass balance for acid-base or kinetic species.

In chromatographic-spectral second-order calibration, such as in the present simulated case, the first three constraints are usually operative: non-negativity in both modes, unimodality for each sub-profile in the time mode, and correspondence between species and samples, knowing that the interferent is absent in the calibration standards. The area correlation constraint is sometimes applied; however, in the present case the analyte sub-profiles in the calibration samples are unique and therefore this constraint is not required. As already explained, trilinearity cannot be applied in chromatography due to the unavoidable lack of reproducibility of elution time profiles. Other constraints such as selectivity or local rank demand a detailed knowledge of the component properties, which is not always possible, especially concerning the interferents.

In what follows, one particular solution for the simulated system described above will be studied which complies with the latter constraints, but is different than the one shown in Figs. 1 and 2. To understand the phenomenon under study, equation (3) is expanded as follows:

$$\mathbf{D}_{aug} = [\mathbf{c}_{aug1} \mid \mathbf{c}_{aug2}]\,[\mathbf{s}_1 \mid \mathbf{s}_2]^T \tag{4}$$

where $\mathbf{c}_{aug1}$ and $\mathbf{c}_{aug2}$ are the two columns of $\mathbf{C}_{aug}$, and $\mathbf{s}_1$ and $\mathbf{s}_2$ the columns of $\mathbf{S}$. The pertinent question is: can one mix $\mathbf{c}_{aug1}$ and $\mathbf{c}_{aug2}$ (and $\mathbf{s}_1$ and $\mathbf{s}_2$) to some extent, and still obtain the same $\mathbf{D}_{aug}$ matrix? One way in which this mixing can be done is by introducing in equation (4) an identity matrix ($\mathbf{I}$) formed by the product of a mixing matrix $\mathbf{T}$ and its inverse (recall that $\mathbf{I} = \mathbf{T}\,\mathbf{T}^{-1}$). The process takes advantage of the fact that multiplying by the identity matrix does not change the mathematical result. One particularly useful form of $\mathbf{T}$ is:

$$\mathbf{T} = \begin{bmatrix} 1 & y \\ x & 1 \end{bmatrix} \tag{5}$$

whose inverse can be easily computed as:

$$\mathbf{T}^{-1} = \frac{1}{1-xy}\begin{bmatrix} 1 & -y \\ -x & 1 \end{bmatrix} \tag{6}$$

Fig. 4 illustrates the above process in a pictorial manner.

Simple matrix algebra leads to the following expanded version of $\mathbf{D}_{aug}$ from equation (4):

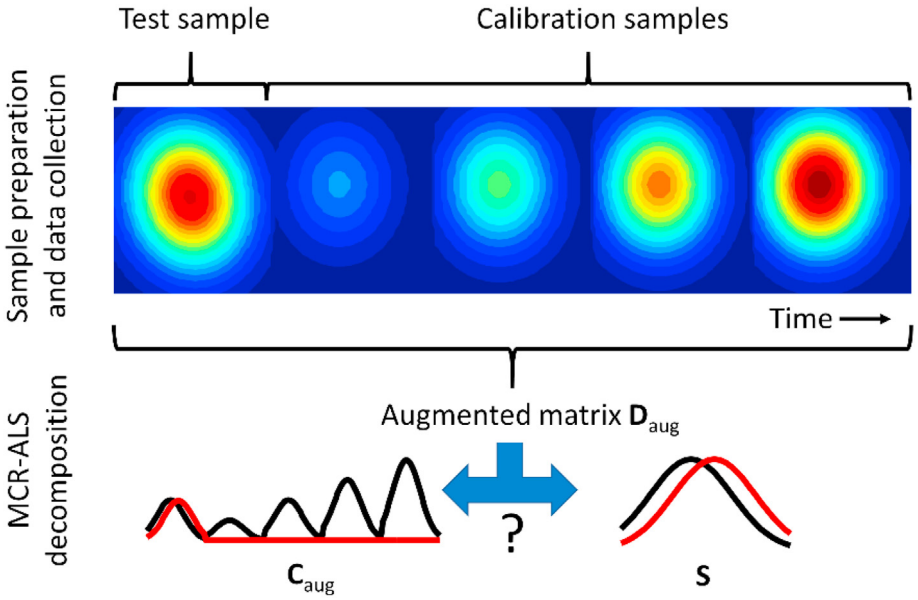

Fig. 3. Schematic representation of a typical second-order multivariate calibration experiment using MCR-ALS for data processing. Top: sample preparation and matrix measurements, leading to the augmented data matrix along the elution time direction. Bottom: bilinear decomposition of the augmented data matrix, leading to two augmented time profiles contained in $\mathbf{C}_{aug}$ and two spectral profiles contained in $\mathbf{S}$. The question mark indicates whether the $\mathbf{C}_{aug}$ and $\mathbf{S}$ matrices retrieved by decomposition are equal or not to the profiles for the analyte (black lines) and the interferent (red lines) which were used to prepare the samples. (For interpretation of the references to colour in this figure legend, the reader is referred to the Web version of this article.)

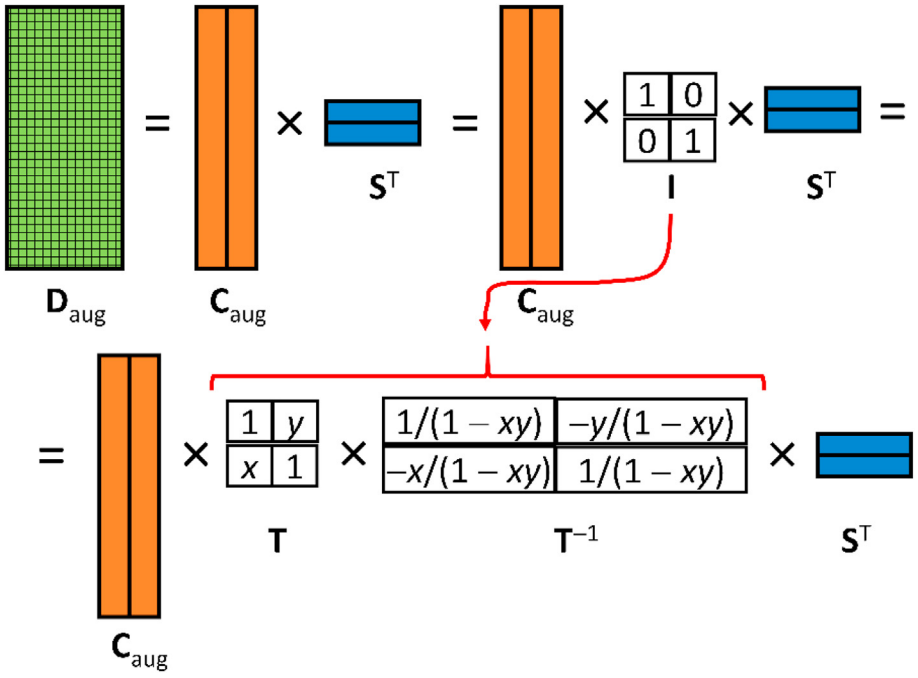

Fig. 4. Pictorial representation of the introduction of the identity matrix $\mathbf{I} = \mathbf{T}\,\mathbf{T}^{-1}$ in equation (4).

$$\mathbf{D}_{aug} = \mathbf{C}_{aug}\ \mathbf{T}\mathbf{T}^{-1}\ \mathbf{S}^T = = \left[\mathbf{c}_{aug1} + x\ \mathbf{c}_{aug2} \middle| \mathbf{c}_{aug2} + y\mathbf{c}_{aug1}\right] [\mathbf{s}_1 - y\ \mathbf{s}_2 | \mathbf{s}_2 - x\mathbf{s}_1]^T \left(\frac{1}{1-xy}\right) \quad (7)$$

As can be seen in equation (7), the analyte and interferent profiles are mixed in both modes, and the parameters x and y control the degree of mixing. Table 1 shows the mixed profiles resulting from two sets of (x,y) values: (1) $x \neq 0, y \neq 0$ and (2) $x \neq 0, y = 0$, along with the ideal solutions $x = 0, y = 0$. As will be shown in the subsequent discussion, the $x \neq 0, y \neq 0$ case corresponds to the use of the non-negativity constraint, the $x \neq 0$, $y = 0$ case corresponds to the use of the non-negativity and correspondence constraints, and the $x = 0$, $y = 0$ corresponds to the trilinear case (Table 1).

The next question to be posed in the present context is: are there values of x and y for which the profiles of equation (7) and

Table 1
Analyte and interferent elution time mode and spectral profiles after mixing the original profiles with the mixing parameters x and y.[a]

	$x \neq 0, y \neq 0$	
Component	Augmented time profile	Spectral profile
1 (analyte)	$\mathbf{c}_{aug1} + x\,\mathbf{c}_{aug2}$	$(\mathbf{s}_1 - y\,\mathbf{s}_2)/(1-xy)$
2 (interferent)	$\mathbf{c}_{aug2} + y\,\mathbf{c}_{aug1}$	$(\mathbf{s}_2 - x\,\mathbf{s}_1)/(1-xy)$
	$x \neq 0, y = 0$	
1 (analyte)	$\mathbf{c}_{aug1} + x\,\mathbf{c}_{aug2}$	$\mathbf{s}_1$
2 (interferent)	$\mathbf{c}_{aug2}$	$\mathbf{s}_2 - x\,\mathbf{s}_1$
	$x = 0, y = 0$	
1 (analyte)	$\mathbf{c}_{aug1}$	$\mathbf{s}_1$
2 (interferent)	$\mathbf{c}_{aug2}$	$\mathbf{s}_2$

[a] The $x \neq 0, y \neq 0$ case corresponds to the use of the non-negativity constraint, the $x \neq 0, y = 0$ case corresponds to the use of the non-negativity and correspondence constraints, and the $x = 0, y = 0$ corresponds to the trilinear case.

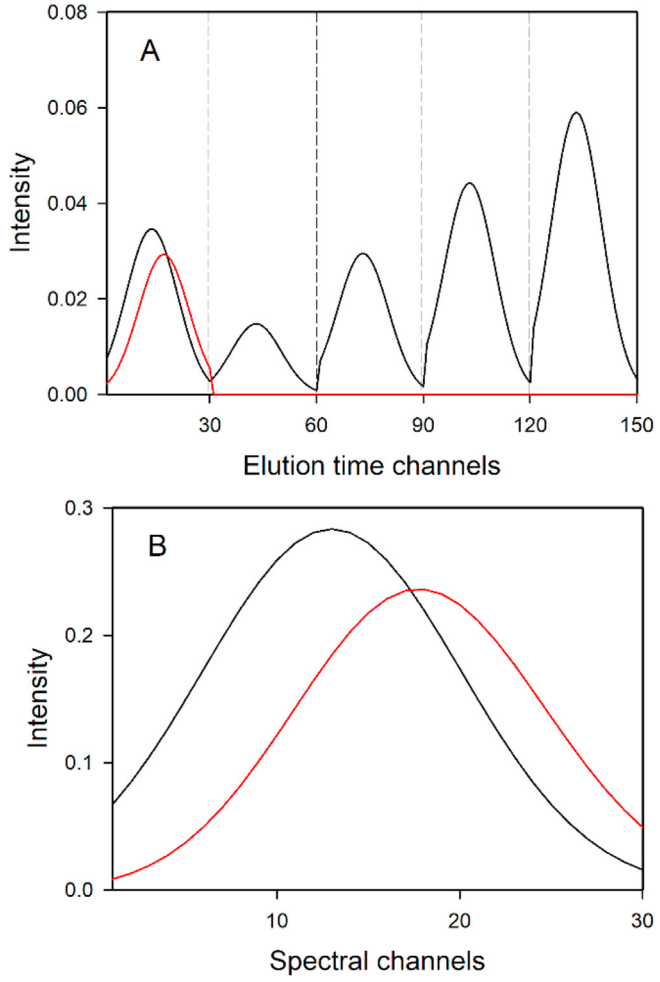

Fig. 5. A) Augmented time profiles for the two components, after mixing the component profiles with $x = 0.2$, $y = 0$ in equation (7). The vertical dashed lines separate the sub-profiles for each sample. B) Spectral profiles. Black lines, analyte of interest, red lines, interferent. (For interpretation of the references to colour in this figure legend, the reader is referred to the Web version of this article.)

Table 1 have chemical meaning? They already satisfy the mathematical requirement of describing a bilinear decomposition of the data matrix $\mathbf{D}_{aug}$, but do they also satisfy chemically sensible constraints?

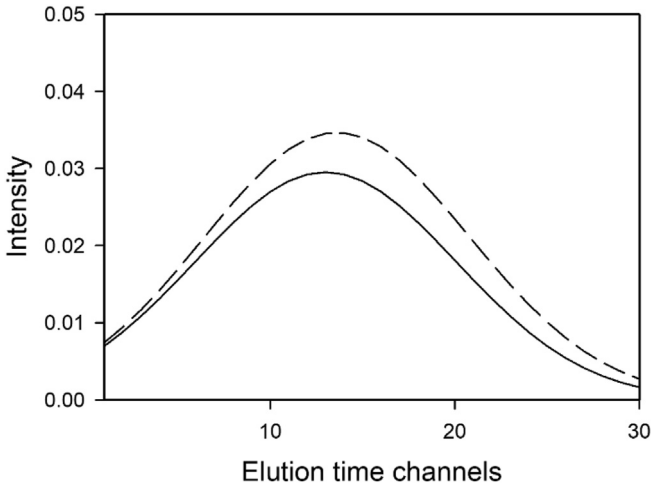

Fig. 6. Elution time sub-profile for the analyte in the original system (black solid line) and after mixing profiles with $x = 0.2$, $y = 0$ in equation (7) (black dashed line).

Let us find the profiles produced by inserting a small value of x, such as $x = 0.2$ in equation (7), keeping $y = 0$. Table 1 shows the profile equations and Fig. 5 plots the result: as can be seen, the new profiles are entirely compatible with the chemical requirements for this system: (1) they are all non-negative, (2) the interferent is absent in the calibration samples, and is only present in the test sample, and (3) the elution time profiles for both components are unimodal.

On close inspection of Fig. 5A regarding the analyte, which is of primary interest from the analytical point of view, none of its calibration sub-profiles in the time direction changes, because the interferent is absent in these samples, and therefore the mixing does not affect them. Likewise, its spectrum remains unchanged, because $y = 0$ [see equation (7) and Table 1]. The only, albeit critical change, takes place in the analyte sub-profile in the test sample, due to the mixing effect brought about by x [see equation (7) and Table 1]. Fig. 6 compares the original and modified analyte sub-profiles in the test sample in the time mode: it is apparent that there is a change in shape, and most importantly, in area. If the decomposition process ends in the modified sub-profile instead of in the original one, then the estimated analyte concentration in the test sample would not be accurate.

The above discussion means that the augmented data matrix can equivalently be described as containing the signals from the constituents described by the profiles in Fig. 1 or those in Fig. 5. There is no way to distinguish one situation from the other one, since both obey the rules of the game, and the only usually known property (the analyte spectrum $\mathbf{s}_1$) is the same in both sets of profiles. What is worse, there might be many other values of x and y satisfying the constraints, leading to additional, equivalent sets of profiles satisfying the bilinear decomposition conditions and chemically sensible constraints.

This is the real meaning behind the expression “rotational ambiguity”. The fact that the phenomenon is called ambiguity is easily understandable. But why is it called “rotational”? In linear algebra, multiplication by a rotation matrix and then by its inverse leaves the result unchanged. Since in equation (4) multiplication by $\mathbf{T}\,\mathbf{T}^{-1}$ leaves $\mathbf{D}_{aug}$ unchanged, an analogy led to the use of the term “rotational ambiguity”.

6. The range of non-negative feasible solutions

How to calculate the range of x and y values satisfying the bilinear decomposition according to equation (3) and the chemical

constraint of non-negativity? Although analytical solutions exist for this particular problem [8], an easily understandable way to answer this question is to scan many values of (*x*,*y*) pairs, and for each of them find the resulting profiles and then decide whether they obey the non-negativity rule. This method is called grid search [8].

To make the process automatic, it is usual to follow these steps for each pair of values of *x* and *y*: (1) find the rotated $\mathbf{C}_{aug}$ and **S** matrices according to equation (7) and (2) replace all their negative elements by zeros to comply with non-negativity, (3) multiply the modified (non-negative) time and spectral matrices to produce a $\mathbf{D}_{auggs}$ matrix (gs for grid search), and (4) study the difference between $\mathbf{D}_{auggs}$ and $\mathbf{D}_{aug}$, because if they are identical, the rotated solutions are as good as the original ones, but if $\mathbf{D}_{auggs}$ differs from $\mathbf{D}_{aug}$, it implies that the non-negative constraint is not being obeyed.

A usual measure of the degree of departure of $\mathbf{D}_{auggs}$ from $\mathbf{D}_{aug}$ is the sum-of-squared residuals (SSR):

$$\mathrm{SSR} = \sum_{j=1}^{J} \sum_{i=1}^{I} [d_{auggs}(i,j) - d_{aug}(i,j)] \tag{8}$$

Notice that the above procedure involving the replacement of negative elements by zeros is adequate for noiseless matrices. In this case, if $\mathbf{D}_{auggs}$ contains negative elements, replacing them by zeros will lead to a substantial SSR value, meaning that the specific profiles leading to $\mathbf{D}_{auggs}$ do not belong to the set of feasible solutions.

A plot of the logarithm of SSR as a function of *x* and *y* allows one to visualize the range of values satisfying the bilinear decomposition and non-negative constraint. This plot is shown in Fig. 7: the region where $\mathbf{D}_{auggs}$ is essentially identical to $\mathbf{D}_{aug}$ (within the digital machine accuracy) can be easily appreciated.

The region of minimum SSR in Fig. 7 can be described as a "flat" rectangle, with the following boundaries: $-0.30 < x < +0.32$ and $0 < y < +0.30$. There are no local minima, and all solutions within

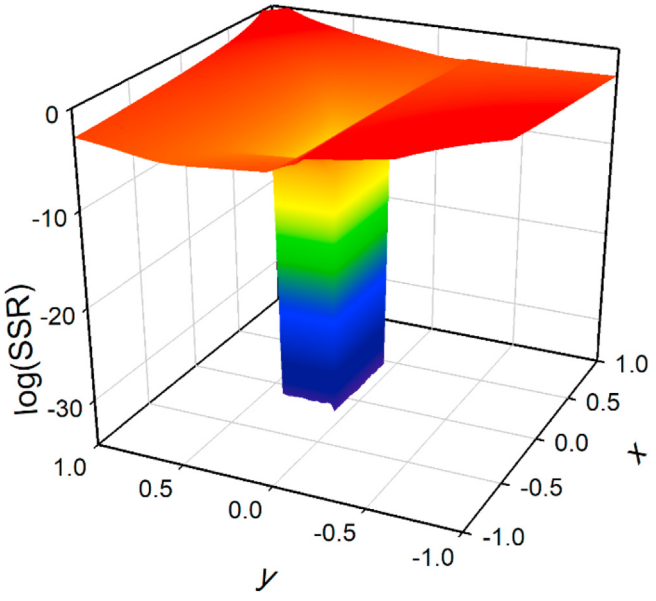

Fig. 7. Plot of the logarithm of the sum-of-squared residuals [log (SSR)] corresponding to the difference of the original augmented data matrix and the one resulting from mixing the analyte and interferent profiles according to equation (7), as a function of the mixing parameters *x* and *y*. The only applied constraint is non-negativity. The value of log (SSR) for $x = 0$, $y = 0$ which is $-\infty$, has been replaced by -33.5, close to the neighbouring values.

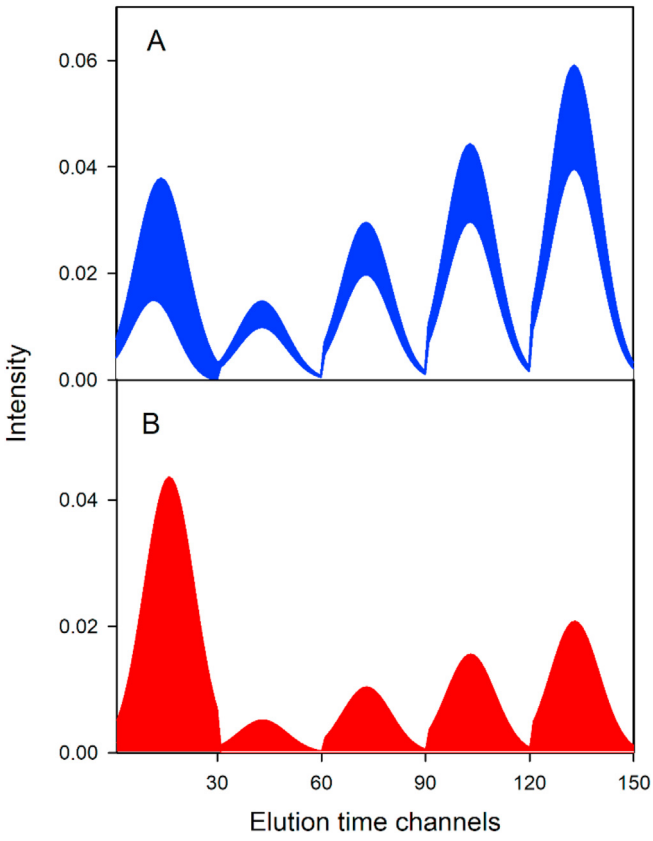

Fig. 8. A) Augmented elution time profiles for the analyte for all feasible values of the mixing parameters *x* and *y* in equation (7). B) Feasible interferent augmented time profiles. The only applied constraint is non-negativity. Notice the presence of the interferent in the calibration samples in B).

the flat minimum region are equally acceptable (for the ideal situation with no noise present). They are called the feasible solutions for the bilinear decomposition. The profiles belonging to these feasible solutions are collected in Figs. 8 and 9 for both constituents of this system under the non-negativity constraint. Inspection of Fig. 8B reveals that if only the non-negativity constraint is applied, there are solutions which do not fulfil another important requirement for this system: the correspondence constraint. Some solutions contain the interferent in the calibration samples, which is not in accordance with the preparation of the calibration samples. Therefore, it is apparent that by imposing further constraints to the decomposition beyond non-negativity, the range of feasible solutions can be reduced.

The range of feasible solutions discussed above is displayed in what theoreticians call the real space, i.e., the space represented by the real variables: time and wavelength channels in the present case. A simplified view can be obtained if the solutions are projected onto the space spanned by principal component analysis (PCA) of the augmented data matrix, allowing to represent each solution as a point in the latter space. All feasible points form a line segment for two-component systems, a surface for three components and a volume for four components. The set of feasible points have been called the area of feasible solutions (AFS), although strictly speaking an area only corresponds to the three-component case. The construction and analysis of these plots started with the work of Lawton and Sylvestre [10] and subsequently of Borgen [31]. Further details on the theory behind Borgen plots can be found in ref [32].

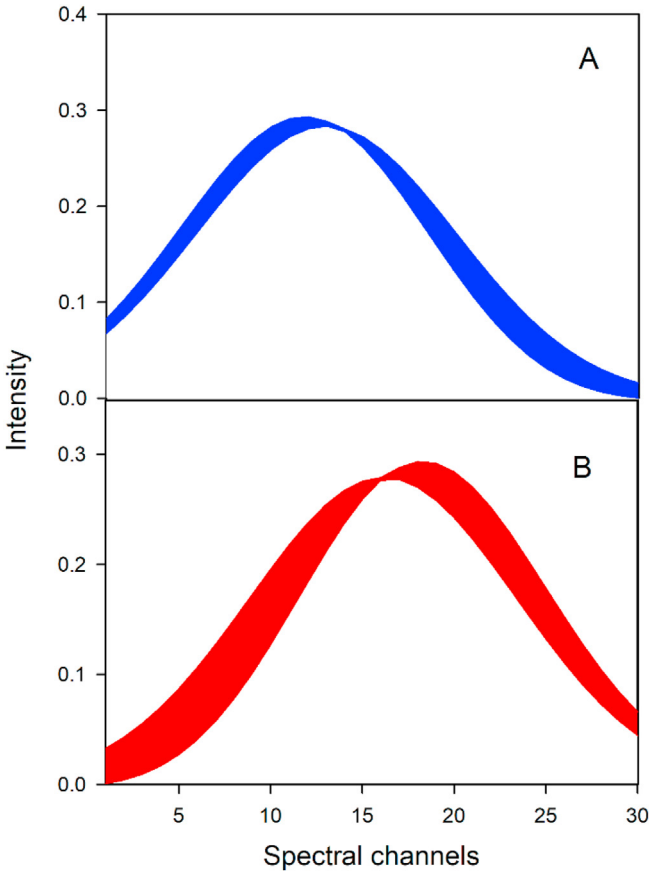

Fig. 9. A) Spectral profiles for the analyte for all feasible values of the mixing parameters x and y in equation (7). B) Feasible interferent spectral profiles. The only applied constraint is non-negativity.

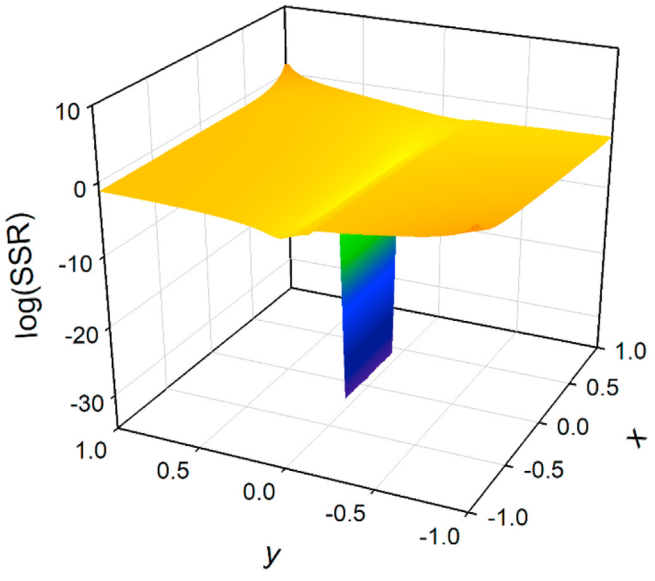

Fig. 10. Logarithm of the sum-of-squared residuals [log (SSR)] corresponding to the difference of the original augmented data matrix and the one resulting from mixing the analyte and interferent profiles according to equation (7), as a function of the mixing parameters x and y. Applied constraints: non-negativity and species correspondence.

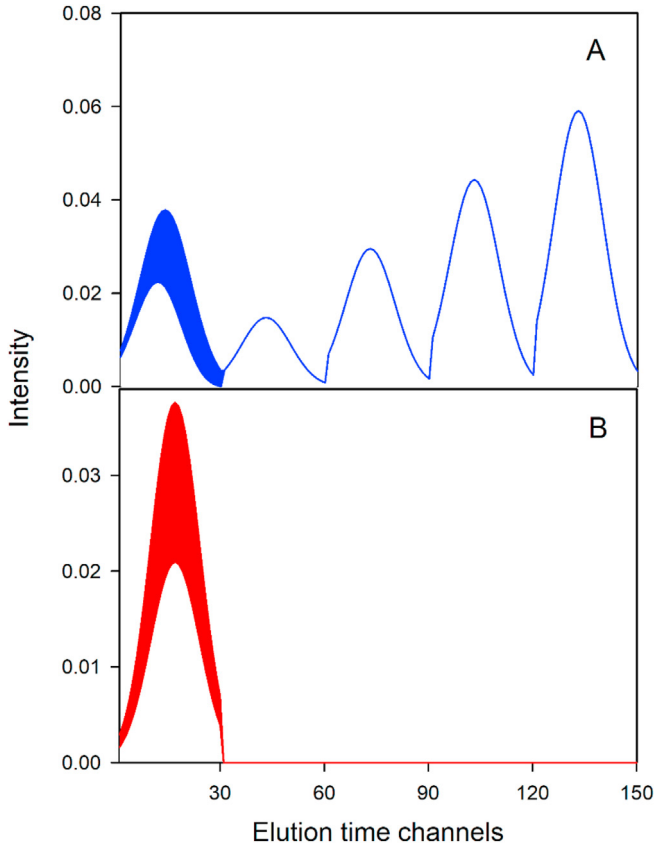

Fig. 11. A) Augmented elution time profiles for the analyte for all feasible values of the mixing parameters x and y in equation (7). B) Feasible interferent augmented time profiles. Applied constraints: non-negativity and species correspondence.

7. Adding the correspondence constraint

To apply both non-negativity and correspondence to the grid search study, a procedure similar to the one described above is implemented, scanning many pairs of values of x and y, and not only setting the negative elements of the rotated matrices to zero, but also setting the elements of the sub-profiles for the interferent in all calibration samples to zero. The latter activity corresponds to applying the species correspondence constraint.

The new plot of log (SSR) as a function of x and y is shown in Fig. 10. The conclusion is that the range of feasible solutions has been reduced from a rectangular region to a segment of a line along $y = 0$, defined by $-0.30 < x < +0.32$. The sets of profiles of both components for the feasible values of x are shown in Figs. 11 and 12, which lead to interesting conclusions. The elution time profiles for the analyte in the calibration samples are unique and do not suffer from rotational ambiguity, which is restricted to the test sample, where the feasible time profiles exhibit different shapes (Fig. 11A). This means that although pure analyte standards have been employed to prepare the calibration samples, and the time profiles in these samples are unique, it does not prevent the appearance of ambiguities in the analyte profile in the test sample. On the other hand, the spectrum of the analyte is unique (Fig. 12A).

With regard to the interferent, Fig. 11B appears to show that there are many different feasible time profiles. However, on close inspection, they all have the same shape, so that after scaling to the same maximum value, they are all identical (recall that scaling is a source of ambiguity, and it is allowed to multiply all time profiles by a number and divide the spectral profiles by the same number).

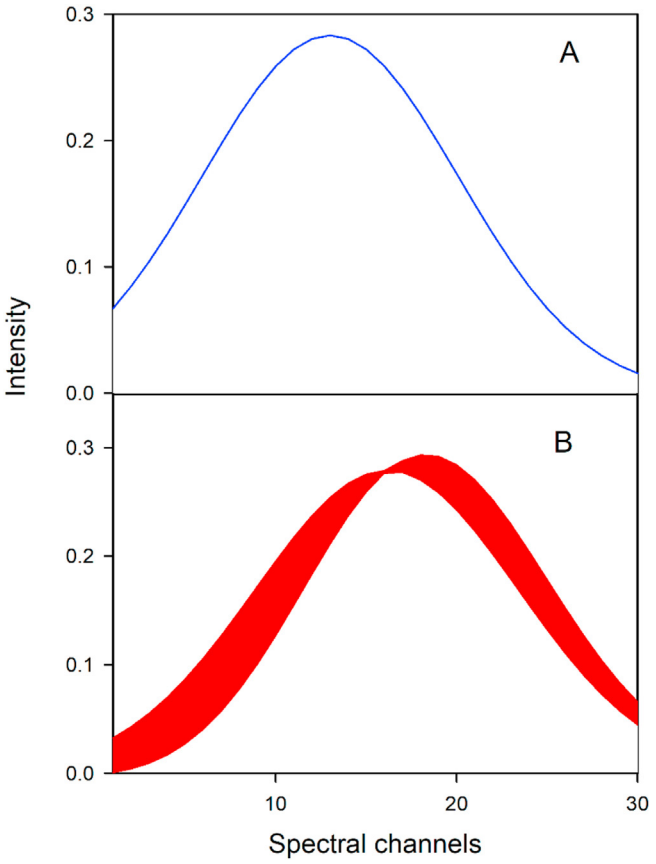

Fig. 12. A) Spectral profiles for the analyte for all feasible values of the mixing parameters x and y in equation (7). B) Feasible interferent spectral profiles. Applied constraints: non-negativity and species correspondence.

This implies scale ambiguity but not rotational ambiguity in the interferent time profile. Finally, the interferent spectra are clearly showing a range of different shapes (Fig. 12B). This complementary relationship of uniqueness in one mode and ambiguity in the other mode for each component is a consequence of the so-called duality principle. For detailed theoretical discussions on the latter concept see refs. [33,34].

The important result is that adding the correspondence constraint to the non-negativity constraint reduces the range of feasible solutions. The present analysis is a highly simplified example showing the meaning of the expression "the application of constraints reduces the range of feasible solutions in MCR decomposition of the augmented data matrix". Finally, notice that even after the application of both constraints, the feasible analyte subprofiles in the test samples display a range of profile areas, which would naturally lead to a range of estimated analyte concentrations, depending of the result of the bilinear decomposition. Since there is no guarantee that MCR-ALS would end at any particular solution, the range of areas in Fig. 11A will be translated into a certain degree of uncertainty in analyte prediction. A method to estimate this uncertainty is discussed below.

8. Where will the MCR-ALS decomposition end?

Suppose an MCR-ALS analysis is started from a given set of initial time and spectral profiles, and the progression from this initial state to the final state is followed on the (x,y) plane of Fig. 10. Since the least-squares phase is driven to the minimum while simultaneously obeying the active constraints (non-negativity and correspondence in the present case), it is natural to expect that this process will first move from any initial point to the line for which $y = 0$. This is because along this line the correspondence constraint is obeyed. Once a point in the latter line is reached, the subsequent ALS steps will be taken in any of three different modes: (1) if the initial value of x is larger than $+0.32$, it will move along the segment to smaller values of x until the extreme value of $+0.32$ is reached, (2) if initial the value of x is smaller than -0.30, it will move along the segment to larger values of x until the extreme value of -0.30 is reached, and (3) if the initial value of x is in the range $-0.30 < x < +0.32$, it will end at that point. These three alternatives are the result of all values within the feasible region being equally acceptable as solutions (see Fig. 13).

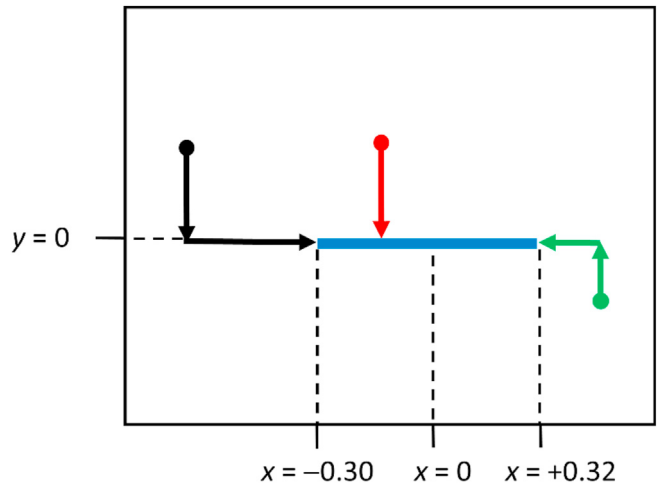

Fig. 13. Motion of the MCR-ALS steps in the (x,y) plane starting from different initial states. Starting from the black circle, the ALS phase first moves to the line with $y = 0$, and then to the segment extreme at $x = -0.30$, $y = 0$. Starting from the green circle, it first moves to the line with $y = 0$, and then to the other segment extreme at $x = 0.32$, $y = 0$. Finally, starting from the red circle, it moves to the line with $y = 0$ and remains there. The blue segment is the region of feasible solutions. (For interpretation of the references to colour in this figure legend, the reader is referred to the Web version of this article.)

It should be noticed that the above discussion corresponds to an ideal case involving noiseless data. In practice, where instrumental noise is always present, the solutions located along the segment will not be identical, and a local minimum will occur. Therefore, for real experimental data, the final solution may differ from the ideal one. Moreover, in this simple example the path corresponding to the intermediate MCR-ALS solutions can be easily illustrated in a two-dimensional plot. However, this becomes increasingly complex for multi-component systems.

In the present case, since the correct solution is the one for $x = 0$, $y = 0$, it is likely that any MCR-ALS initial set of solutions will be

Table 2
Relative difference between maximum and minimum areas of analyte sub-profile in the test sample (ΔA) with respect to the area in the calibration sample with maximum analyte concentration [max(A)], for decreasing ratios between the value of full width at half maximum (FWHM) and peak separation.

FWHM/(peak separation)[a]	% ΔA/max(A)
4	32
3	11
2	3.5
1	0.5

[a] Gaussian profiles are assumed to have the same FWHM in both data modes.

driven to other points, thus leading to the estimation of inaccurate analyte concentrations (Fig. 13). This is a rather extreme example of an unsuccessful analyte protocol with second-order data and MCR-ALS as data processing algorithm. The pure chromatograms and spectra for the analyte and interferent are highly overlapped (Fig. 1), and there are no time or spectral regions for which the signals are selective for the analyte. It was selected to show a rather pessimistic scenario, which is perhaps unlikely but not impossible.

On the other hand, the literature shows a large number of successful analytical developments based on matrix chromatographic data processed with MCR-ALS [35]. In the above example, the analyte and interferent profiles are described by Gaussian lines, both with a ratio of full width at half maximum (FWHM) to the separation of the two maxima of ca. 4. If the degree of overlapping decreases, by decreasing the latter ratio, the extent of rotational ambiguity also decreases. Table 2 shows the progression of the relative difference in areas between the maximum and minimum areas of the analyte sub-profile in the test sample, as the FWHM decreases with respect to the separation between component peaks in both data modes.

9. The trilinearity constraint

Consider the solution for which $x = 0.2$, $y = 0$, which is within the range of feasible solutions complying with both non-negativity and correspondence for the system illustrated in Fig. 1. The four elution time profiles of the analyte in the calibration samples, when scaled so that they all have the same maximum value of 1, are identical (see Fig. 14). This means that all of them have exactly the same shape. However, due to the mixing with the interferent, the shape of the elution time profile for the analyte in the test sample is altered (Fig. 14).

Suppose it is known in advance that, due to the characteristics of the experiment, all analyte profiles in the augmented mode should share the same shape. In certain chromatographic experiments, as in gas chromatography, the elution time profiles are known to be highly reproducible, so it can be assumed that they will all be approximately equal. Likewise, in other experimental techniques outside the chromatography field, as in excitation-emission matrix fluorescence spectroscopy, the shapes of the excitation and of the emission spectra for a given component are known to have the same shape in all samples [15]. What would happen when imposing the constraint that the shapes of all profiles for a given component in the augmented mode in all samples are the same? The result is shown in Fig. 15.

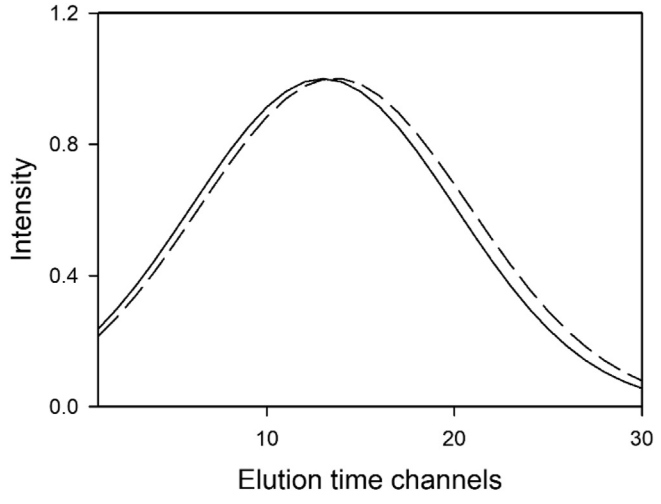

Fig. 14. Black solid line, analyte sub-profiles in the calibration samples, all scaled to a common maximum height of 1. Black dashed line, analyte sub-profile in the test sample, scaled to a maximum height of 1.

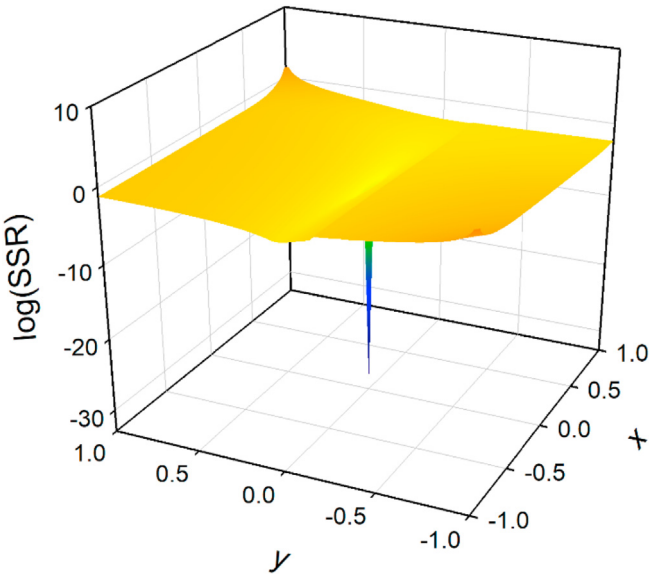

Fig. 15. Plot of the logarithm of the sum-of-squared residuals [log (SSR)] corresponding to the difference of the original augmented data matrix and the one resulting from mixing the analyte and interferent profiles according to equation (7), as a function of the mixing parameters x and y. Applied constraints: non-negativity, species correspondence and trilinearity.

The solution is unique! A single minimum occurs at the correct point $x = 0$, $y = 0$. This constraint is called trilinearity, because this property is found in fluorescence spectroscopy, where the shape of the excitation and emission spectra for a given component is the same in all samples [15]. These data can be mathematically described as depending on three profiles along the elution time, spectral and sample modes. Incidentally, the trilinearity constraint is so strong that in principle it does not require other constraints to achieve uniqueness in the solutions. However, its application in chromatographic matrix data is limited since in principle the elution time profiles is not constant across samples.

For a discussion on uniqueness see refs. [36–41]. These reports provide useful rules for detecting uniqueness in the bilinear decompositions. However, when the solution is not unique, it is necessary to estimate the extent of rotational ambiguity, to quantitatively evaluate its relative impact on the uncertainty in analyte determination.

10. Estimating the concentration uncertainty from rotational ambiguity

A misconception in second-order multivariate calibration with MCR-ALS is that a proper calibration design, involving samples with pure analyte standards, and with partial profile overlapping in both instrumental domains, would lead to unique solutions. The above example has clearly shown that this is not the case: in the presence of interferents, a substantial degree of rotational ambiguity may remain in the bilinear decomposition. Only if the data were trilinear a unique solution would be found; however, chromatographic-spectral second-order data are in principle non-trilinear, due to the sample dependence of elution time profiles. It is thus important to remark that analysts employing second-order multivariate protocols based on chromatographic data, where interferents may appear in the test samples, should always check for the presence of the occurrence of rotational ambiguity in the solutions.

Given that rotational ambiguity may be a ubiquitous problem, it is important to be able to size the degree of uncertainty in the estimation of an analyte concentration brought about by this phenomenon. The grid search methodology described above is a possibility, but unfortunately it is impractical for multi-component systems. Likewise, a number of alternative methods based on comprehensive searches are also impractical. One attractive alternative is to only find two extreme feasible solutions, corresponding to the maximum and minimum value in some function measuring the contribution of a specific component to the overall signal, both satisfying the constraints imposed to the system. The idea was implemented as a non-linear optimization problem under non-linear constraints, using different objective functions, such as: (1) the sum of all elements of the product ($\mathbf{c}_n\ \mathbf{s}_n^T$) [42], (2) the signal contribution function (SCF), defined as the ratio of the 2-norm of the product ($\mathbf{c}_n\ \mathbf{s}_n^T$) to the 2-norm of ($\mathbf{C}\ \mathbf{S}^T$) [43], and (3) the relative component area α, defined as the ratio of the sum of all elements of $\mathbf{c}_n$ to the sum of all elements of $\mathbf{C}$ [44]. The algorithm MCR-BANDS implements the SCF concept in a graphical interface [45], available at www.mcrals.info. The newly developed N-BANDS uses the area-related parameter α for maximization/minimization in the presence of instrumental noise [46], and has been incorporated in the latest version of the graphical user interface MVC2 for second-order multivariate calibration, which is freely available at www.iquir-conicet.gov.ar (MATLAB version) and at https://www.dropbox.com/sh/nruf3lp0ge1gbww/AAAj6r97UBMIhgQmukRGYFPKa?dl=0 (stand-alone compiled version) [47]. Applications of the latter concepts can be found in refs. [48,49].

A literature discussion concerns the question of whether the extreme feasible solutions, computed in any of the three manners discussed above, are able to enclose the full set of feasible solutions, and/or to measure the extent of rotational ambiguity. It appears that this is indeed the case for a two-component system, but may not be the case for more sample components [50]. Recently, however, it became clear that what really matters regarding the estimation of a concentration uncertainty is the area under the analyte profile in the elution time mode. This is because the analyte concentration in each sample is proportional to the area of the corresponding sub-profile in the augmented mode, provided all spectra are normalized to unit 2-norm, as discussed above. Under this premise, it is possible to estimate the maximum and minimum areas for the analyte sub-profile in the test sample. The points corresponding to these two extremes may or may not lie in the border of the region of feasible solutions, however, they provide a good measure of the range of areas to be expected for the analyte sub-profile in the test sample, and hence of the range of estimated concentrations for this particular analyte.

Once the maximum and minimum analyte areas are estimated, the difference between the latter can be converted to concentration units [51]:

$$\delta_{RA} = \frac{\max(a_{test}) - \min(a_{test})}{s} \tag{9}$$

where max (a_{test}) and min (a_{test}) are the minimum and maximum areas under the analyte concentration profiles in the test sample, and s is the slope of the pseudo-univariate analyte calibration graph. The parameter δ_{RA} is shown in Fig. 16 as a source of rotational ambiguity uncertainty, compared to two other common uncertainty sources, such as random instrumental noise propagated to estimated concentrations and concentration bias. It has been shown that the root mean square error due to rotational ambiguity uncertainty ($RMSE_{RA}$) is given by the following range of values [51]:

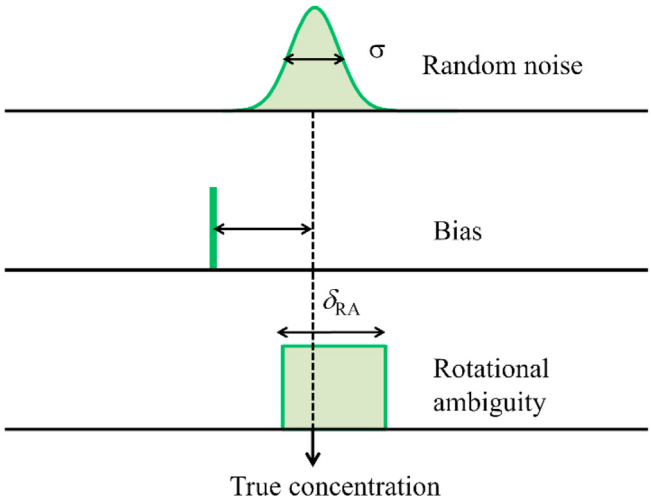

Fig. 16. Schematic representation of the uncertainty in estimated analyte concentration stemming from the propagation of random noise, concentration bias and rotational ambiguity. Reproduced with permission from ref. [51] (American Chemical Society).

$$RMSE_{RA} = \left[\frac{1}{\sqrt{12}} \times \delta_{RA}; \frac{1}{\sqrt{3}} \times \delta_{RA}\right] \tag{10}$$

The parameter $RMSE_{RA}$ has been described as a new figure of merit to be reported in all second-order multivariate protocols employing bilinear decomposition of matrix data. The new version of the MVC2 software mentioned above estimates the range of $RMSE_{RA}$ values, in % with respect to the mean calibration concentration of the analyte of interest.

In the example discussed above, if non-negativity and correspondence are applied as constraints, the extreme profiles can be estimated in both data modes corresponding to maximum and minimum relative area α under the elution time profiles using the MCR-BANDS algorithm. Notice that the spectral profiles for both components are normalized so that they have unit 2-norm for both components during the optimization procedure leading to the extreme values of α. The result is shown in Fig. 17 for the rotationally ambiguous analyte and interferent profiles in the test sample, and for the interferent spectrum. Fig. 17 also shows the grid search results superimposed with the extreme profiles, indicating that the latter enclose the feasible profiles in both data modes. However, as mentioned above, this enclosing phenomenon is not general.

By maximization and minimization of the relative analyte area α, the difference in extreme area values is estimated as 0.32 units, which is 32% of the maximum value for the calibration samples (1 unit, corresponding to the sample with analyte at unit concentration). This agrees with the value given in Table 2, estimated from the grid search approach. On the other hand, the range of $RMSE_{RA}$ values for this simulated system, according to equation (10) is 0.09–0.18 concentration units. In relative terms with respect to the mean calibration concentration (0.62 units), these values represent between 15 and 30% of relative error of prediction (REP%), which can be considered substantial.

11. An experimental example

In this section an experimental example will be described, which involved the determination of ten polycyclic aromatic hydrocarbons in water samples at very low concentrations, in the

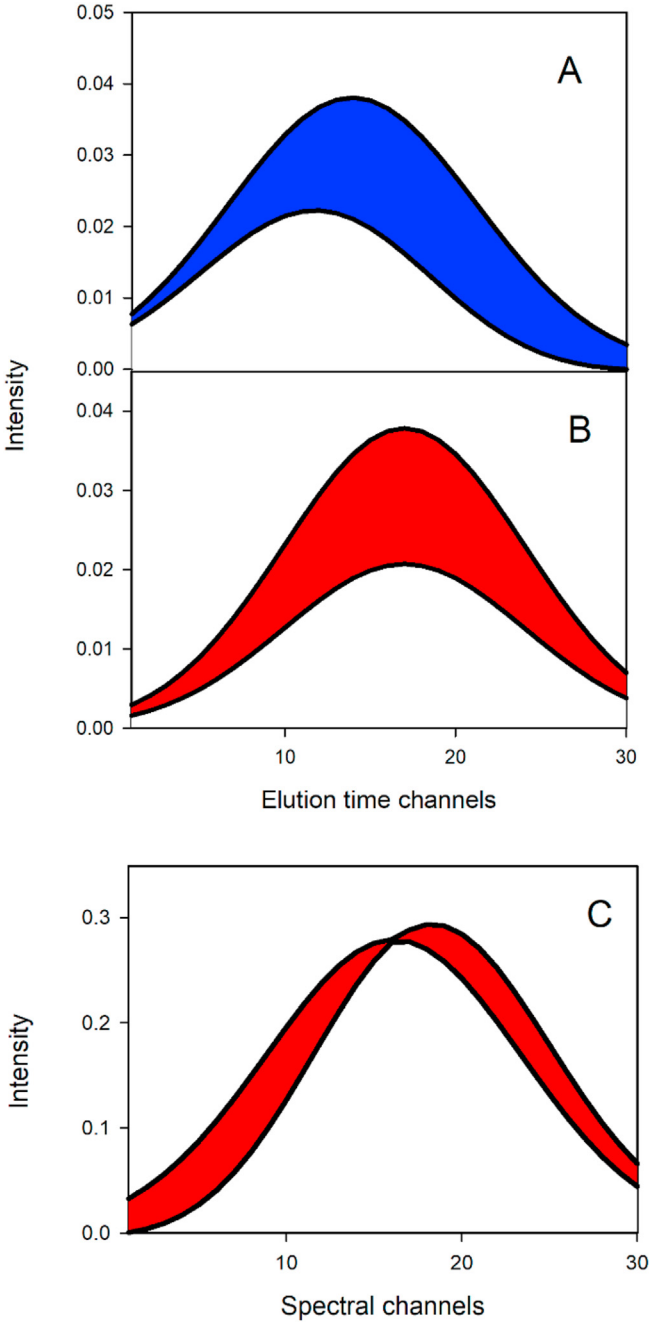

Fig. 17. Thick black lines: extreme profiles for maximum and minimum relative areas calculated with MCR-BANDS. A) Analyte in the time mode for the test sample. B) Interferent in the time mode for the test sample. C) Interferent in the spectral mode. The blue and red areas are those from Figs. 11 and 12, as estimated by grid search. (For interpretation of the references to colour in this figure legend, the reader is referred to the Web version of this article.)

presence of uncalibrated interferents [52]. The analytical protocol was developed using high-performance liquid chromatography with fast-scanning fluorescence detection, coupled to MCR-ALS data processing. Fig. 18 shows the elution time and spectral profiles retrieved by the latter model from the analysis of a typical test sample, where the complexity of the analytical problem is apparent.

The analysis of a test sample set, comprising additional samples to that shown in Fig. 18, rendered reasonable analytical results, with relative errors of prediction for all analytes in the range 5–25%. At

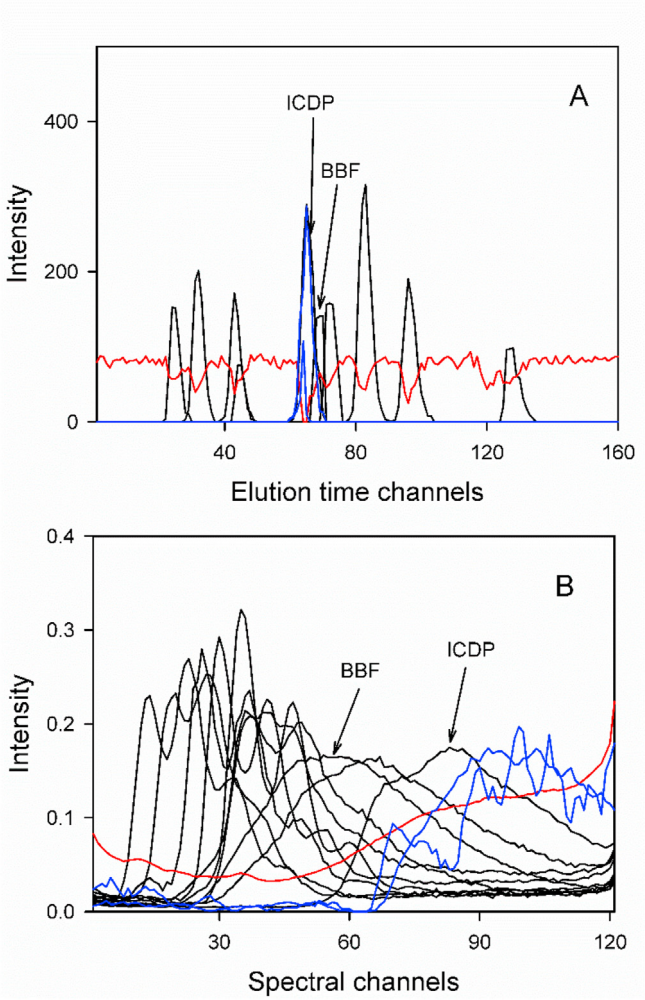

Fig. 18. A) Retrieved MCR-ALS elution time profiles in a typical test sample for the ten analytes (black lines, with names of the most compromised analytes indicated), the interferents (blue lines) and a background signal (red line) when studying a typical test sample. B) The corresponding spectral profiles, with the same colouring scheme and labels as in A). (For interpretation of the references to colour in this figure legend, the reader is referred to the Web version of this article.)

the time this protocol was developed, no rotational ambiguity effects were considered. Notice that it would be highly impractical to employ the grid search or similar methodologies for assessing the rotational ambiguity in a system with 13 components. The latter analysis, made with the non-linear optimization tool included in the MVC2 software mentioned above for estimating the maximum and minimum component areas in the test sample, provides $RMSE_{RA}$ ranges from 2-4% to 5–10%. This implies that in the developed protocol the relative impact of rotational ambiguity was not significant. Fig. 19 shows the sub-profiles in the elution time mode corresponding to maximum and minimum areas for the most compromised analytes due to time overlapping with the interferents, i.e., indeno [*c,d*]pyrene (ICDP) and benzo [*b*]fluoranthene (BBF).

The result suggests a small degree of rotational ambiguity for these two analytes, which can be estimated as leading to $RMSE_{RA}$ ranges of 2.5–5% and 3–6% respectively. Fig. 20 shows the output of the software MVC2 after MCR-ALS decomposition and selection of the analyte ICDP. The univariate calibration graph appears to be satisfactory. After clicking in the "Feasible profiles" button, Fig. 21 is created, with the extreme feasible profiles in both modes

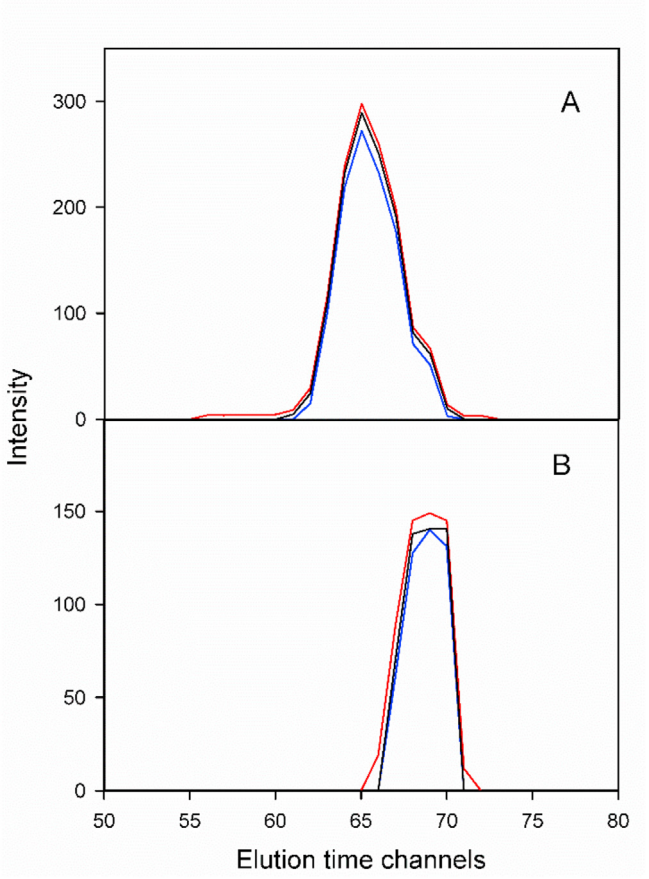

Fig. 19. Elution time profiles retrieved by MCR-ALS (black lines) and extreme feasible profiles corresponding to maximum (red lines) and minimum (blue lines) relative area α, for a typical test sample of the experimental system. A) Indeno [*c,d*]pyrene (ICDP). B) Benzo [*b*]fluoranthene (BBF). (For interpretation of the references to colour in this figure legend, the reader is referred to the Web version of this article.)

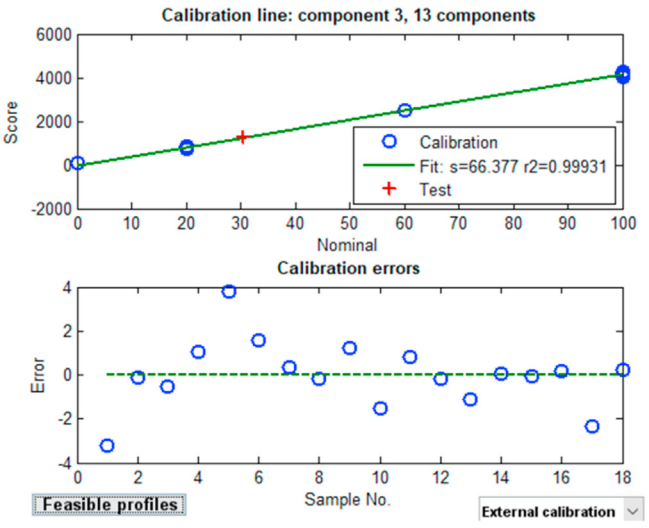

Fig. 20. Screen of the MVC2 software, produced after MCR-ALS processing of a typical test sample of the experimental system. Top, univariate calibration graph for component 3 (ICDP) built with the analyte scores against nominal calibration concentrations. The red cross is the sample score interpolated in the calibration line. Bottom, concentration calibration errors vs. sample number. The button on the bottom left allows one to estimate the extreme feasible profiles and the analyte concentration uncertainty derived from rotational ambiguity. (For interpretation of the references to colour in this figure legend, the reader is referred to the Web version of this article.)

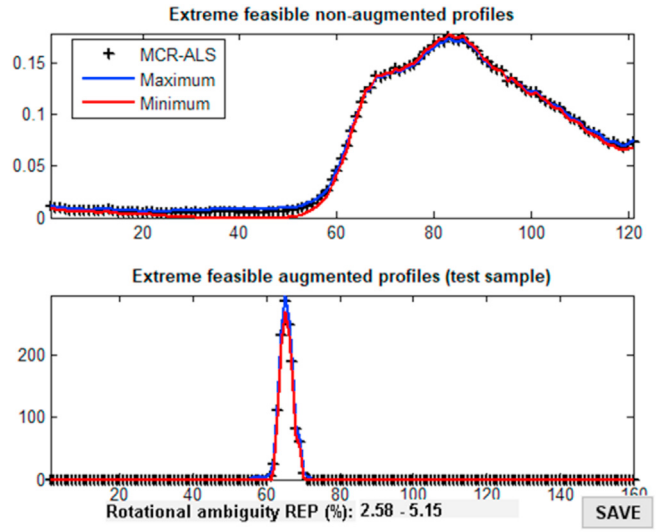

Fig. 21. Screen of the MVC2 software after pressing the button "Feasible profiles" in Fig. 19. Top, extreme spectral profiles. Bottom, extreme concentration profiles in the test sample. The black crosses indicate the MCR-ALS solution.

corresponding to maximum and minimum relative area α, superimposed to the MCR-ALS solution. The range of relative error of prediction (REP%) is indicated below the profile plot. Detailed instructions as to how these data are processed using MVC2 can be found in the software manual and also in ref. [15].

12. Successful protocols even with substantial rotational ambiguity

MCR-ALS requires a starting point for the least-squares minimization phase, consisting of an initial approximation to the solution, which is then refined and driven by the active constraints to the final solution. There are various approximation methods available for estimating the properties of pure sample components that can be used to start MCR-ALS. The reader may find a description of these resources in the literature [1,2,53–57].

The initialization issues regarding rotational ambiguity are better illustrated with a personal story. In the period 2008–2010, the present author published, in cooperation with other colleagues, some analytical developments using matrix data which showed the same component profiles in one of the instrumental modes [58,59]. The good news was that the analyte content could be successfully determined in the presence of interferents, although the rotational ambiguity issue was not considered in these reports.

In 2013, a research group from Iran showed that the latter systems had a substantial degree of rotational ambiguity. Basically, the message was that our estimated analyte concentrations should display a rather large degree of uncertainty [60]. Then in 2017, during a meeting at Newcastle, Australia, the issue was discussed with one of the authors of ref. [60] and other experts in rotational ambiguity. The conclusion was clear: "this calls for an explanation". Why would MCR-ALS give good analytical results when theory indicated otherwise?

Some attempts to reconcile these seemingly contradictory facts were recently reported [61,62]. The idea was that by starting from a certain initial point, MCR-ALS would end at the border of the region of feasible solutions. If the feasible region is a segment of a line, as in the simulated example discussed above, and the right solution is located in one of the extremes of the segment, the MCR-ALS decomposition can be driven to that extreme point, allowing the

analyte content in the test samples to be correctly estimated. It appears that this occurred in our rotationally ambiguous protocols of refs. [58,59]. The key is that if the correct solution is buried inside the region of feasible solutions, it would be unreachable from outside this region, and no starting initialization will provide the correct analyte concentration, unless one knows the right solution from the start, which is seldom possible. Conversely, if the right solution is in the borders, then there is a chance that a good initialization will converge to that point. The condition that needs to be fulfilled for achieving this latter situation is that a selective region should exist for the analyte in the spectral mode [62]. In this case, initialization should be done with concentration profiles estimated at the purest spectral variables, because lower correlation is present in the spectral mode than in the concentration mode [62]. The subject has also been discussed in the framework of MCR-ALS processing of first-order data [63], with the aim of developing an interference-free calibration, achieving the second-order advantage [64]. For two-component systems, the conditions for successful resolution are analogous to those for second-order data with full profile overlapping in one of the data modes.

As a bonus, another collaboration resulted in an alternative protocol to achieve uniqueness in the case of complete profile overlapping in one data mode [65]. It involves the addition, to the calibration set, of samples having known analyte concentrations and the expected interferents to appear in future samples. Imposing the area of the analyte sub-profile in these added samples to reflect their known analyte concentrations led to unique solutions. However, this requires the knowledge and availability of the interferents, which is not always possible.

13. Conclusion

When facing an analytical system where substantial rotational ambiguity remains in the MCR-ALS solutions, due to profile overlapping between the analyte and an uncalibrated interferent in test samples, there are two apparently opposite views: the pessimistic and the optimistic ones.

According to the pessimistic one, all solutions within the range of feasible solutions are equally possible, and thus there is no guarantee, for a given analytical system, that a particular set of starting values will lead to the correct solution, with more probability than to any of the infinite solutions within the feasible region. “Correct” means the solution leading to accurate analyte quantitation in a set of interfering samples. There is no alternative but to report that analyte quantitation is uncertain, and to estimate the degree of uncertainty.

However, it is a fact that various analytical systems have been experimentally developed, in which substantial rotational ambiguity exists, yet the experimental results confirm that accurate analyte quantitation is possible. Thus, an alternative, optimistic view of the phenomenon exists, in the sense that by selecting a given method of estimating starting values, the least-squares phase of MCR will be driven by the applied constraints to the correct solution. This explains why certain experimental protocols, which are apparently destined to fail, have indeed been successful in quantitating analytes in test samples with interferents.

In sum, it is apparent that a second-order multivariate calibration protocol developed by processing the data with MCR-ALS will be successful if: (1) the degree of rotational ambiguity is zero or very small, or (2) the degree of rotational ambiguity is significant, but the selected initialization state and applied constraints drive MCR-ALS to the correct chemical solution.

In any case, the message from the present tutorial is directed to analytical chemists measuring second-order data and processing them with multivariate curve resolution, with the aim of analyte quantitation: the degree of rotational ambiguity and its impact on the uncertainty in estimated analyte concentrations need to be assessed and reported.

Declaration of competing interest

The authors declare that they have no known competing financial interests or personal relationships that could have appeared to influence the work reported in this paper.

Acknowledgments

Financial support from Universidad Nacional de Rosario, Consejo Nacional de Investigaciones Científicas y Técnicas (CONICET) and Agencia Nacional de Promoción Científica y Tecnológica (ANPCyT, Project No. PICT 2016−1122) are gratefully acknowledged.

References

[1] M. Maeder, Evolving factor analysis for the resolution of overlapping chromatographic peaks, Anal. Chem. 59 (1987) 527−530.
[2] M. Mader, A.D. Zuberbuehler, Evolving factor-analysis for the resolution of overlapping chromatographic peaks, Anal. Chim. Acta 181 (1986) 287−291.
[3] R. Tauler, Multivariate curve resolution applied to second order data, Chemometr. Intell. Lab. Syst. 30 (1995) 133−146.
[4] R. Tauler, M. Maeder, A. de Juan, Multiset data analysis: extended multivariate curve resolution, in: S. Brown, R. Tauler, B. Walczak (Eds.), Comprehensive Chemometrics, vol. 2, Elsevier, Oxford, 2009, pp. 473−505.
[5] R. Tauler, M. Maeder, A. de Juan, Multiset data analysis: extended multivariate curve resolution, in: S. Brown, R. Tauler, B. Walczak (Eds.), Comprehensive Chemometrics, Second Edition, Chemical and Biochemical Data Analysis, vol. 2, Elsevier, Oxford, 2020, pp. 305−336 (Chapter 2).15.
[6] R. Tauler, A. de Juan, Multivariate curve resolution for quantitative analysis, in: A. Muñoz de la Peña, H.C. Goicoechea, G.M. Escandar, A.C. Olivieri (Eds.), Data Handling in Science and Technology vol. 29, Elsevier, Amsterdam, 2015, pp. 247−292. Fundamentals and Analytical Applications of Multiway Calibration.
[7] K.S. Booksh, B.R. Kowalski, Theory of analytical chemistry, Anal. Chem. 66 (1994) 782A−791A.
[8] A. Golshan, H. Abdollahi, S. Beyramysoltan, M. Maeder, K. Neymeyr, R. Rajkó, M. Sawall, R. Tauler, A review of recent methods for the determination of ranges of feasible solutions resulting from soft modelling analyses of multivariate data, Anal. Chim. Acta 911 (2016) 1−13.
[9] M. Sawall, H. Schröder, D. Meinhardt, K. Neymeyr, On the ambiguity underlying multivariate curve resolution methods, in: S. Brown, R. Tauler, B. Walczak (Eds.), Comprehensive Chemometrics, Second Edition, Chemical and Biochemical Data Analysis, vol. 2, Elsevier, Oxford, 2020, pp. 199−231 (Chapter 2).12.
[10] W.H. Lawton, E.A. Sylvestre, Self modeling curve resolution, Technometrics 13 (1971) 617−633.
[11] H. Abdollahi, M. Maeder, R. Tauler, Calculation and meaning of feasible band boundaries in multivariate curve resolution of a two-component system, Anal. Chem. 81 (2009) 2115−2122.
[12] R. Rajkó, Additional knowledge for determining and interpreting feasible band boundaries in self-modeling/multivariate curve resolution of two-component systems, Anal. Chim. Acta 661 (2010) 129−132.
[13] R. Rajkó, Some surprising properties of multivariate curve resolution-alternating least squares (MCR-ALS) algorithms, J. Chemometr. 23 (2009) 172−178.
[14] R. Rajkó, Studies on the adaptability of different Borgen norms applied in self-modeling curve resolution (SMCR) method, J. Chemometr. 23 (2009) 265−274.
[15] G.M. Escandar, A.C. Olivieri, Practical Three-Way Calibration, Elsevier, Waltham (US), 2014.
[16] J.A. Arancibia, P.C. Damiani, G.M. Escandar, G.A. Ibañez, A.C. Olivieri, A review on second- and third-order multivariate calibration applied to chromatographic data, J. Chromatogr. B 910 (2012) 22−30.
[17] L. Xu, L.J. Tang, C.B. Cai, H.L. Wu, G.L. Shen, R.Q. Yu, J.H. Jiang, Chemometric methods for evaluation of chromatographic separation quality from two-way data—a review, Anal. Chim. Acta 613 (2008) 121−134.
[18] A.C. Olivieri, Second-order multivariate calibration with the extended bilinear model: effect of initialization, constraints, and composition of the calibration set on the extent of rotational ambiguity, J. Chemometr. 34 (2019), e3130.
[19] A.C. Olivieri, R. Tauler, The effect of data matrix augmentation and constraints in extended multivariate curve resolution−alternating least squares, J. Chemometr. 31 (2017) e2875.
[20] E. Tavakkoli, H. Abdollahi, P.J. Gemperline, Soft-trilinear constraints for improved quantitation in multivariate curve resolution, Analyst 145 (2020) 223−232.

[21] M. Sawall, N. Rahimdoust, C. Kubis, H. Schröder, D. Selent, D. Hess, H. Abdollahi, R. Franke, A. Börner, K. Neymeyr, Soft constraints for reducing the intrinsic rotational ambiguity of the area of feasible solutions, Chemometr. Intell. Lab. Syst. 14 (2015) 140–150.
[22] M. Alinaghi, R. Rajkó, H. Abdollahi, A systematic study on the effects of multi-set data analysis on the range of feasible solutions, Chemometr. Intell. Lab. Syst. 153 (2016) 22–32.
[23] M. Ghaffari, H. Abdollahi, A conceptual view to the area correlation constraint in multivariate curve resolution, Chemometr. Intell. Lab. Syst. 189 (2019) 121–129.
[24] N. Omidikia, S. Beyramysoltan, J. Mohammad Jafari, E. Tavakkoli, M. AkbariLakeh, M. Alinaghi, M. Ghaffari, S. Khodadadi Karimvand, R. Rajko, H. Abdollahi, Closure constraint in multivariate curve resolution, J. Chemometr. 32 (2017) 1–15.
[25] M.A. Lakeh, H. Abdollahi, P.J. Gemperline, Soft known-value constraints for improved quantitation in multivariate curve resolution, Anal. Chim. Acta 1105 (2020) 64–73.
[26] S. Beyramysoltan, H. Abdollahi, R. Rajkó, Newer developments on self-modeling curve resolution implementing equality and unimodality constraints, Anal. Chim. Acta 827 (2014) 1–14.
[27] S. Beyramysoltan, R. Rajkó, H. Abdollahi, Investigation of the equality constraint effect on the reduction of the rotational ambiguity in three-component system using a novel grid search method, Anal. Chim. Acta 791 (2013) 25–35.
[28] R. Tauler, Multivariate curve resolution of multiway data using the multilinearity constraint, J. Chemometr. (2021), https://doi.org/10.1002/cem.3279 (in press).
[29] M. Bayat, M. Marín-García, J.B. Ghasemi, R. Tauler, Application of the area correlation constraint in the MCR-ALS quantitative analysis of complex mixture samples, Anal. Chim. Acta 1113 (2020) 52–65.
[30] A.C. de Oliveira Neves, R. Tauler, K.M.G. de Lima, Area correlation constraint for the MCR– ALS quantification of cholesterol using EEM fluorescence data: a new approach, Anal. Chim. Acta 937 (2016) 21–28.
[31] O.S. Borgen, B.R. Kowalski, An extension of the multivariate component-resolution method to three components, Anal. Chim. Acta 174 (1985) 1–26.
[32] R. Rajkó, K. István, Analytical solution for determining feasible regions of self-modeling curve resolution (SMCR) method based on computational geometry, J. Chemometr. 19 (2005) 448–463.
[33] R.C. Henry, Duality in multivariate receptor models, Chemometr. Intell. Lab. Syst. 77 (2005) 59–63.
[34] R. Rajko, Natural duality in minimal constrained self modeling curve resolution, J. Chemometr. 20 (2006) 164–169.
[35] G.M. Escandar, A.C. Olivieri, Multi-way chromatographic calibration - a review, J. Chromatogr. A 1587 (2019) 2–13.
[36] R. Manne, On the resolution problem in hyphenated chromatography Chemom, Intell. Lab. Syst. 27 (1995) 89–94.
[37] E. Tavakkoli, R. Rajkó, H. Abdollahi, Duality based direct resolution of unique profiles using zero concentration region information, Talanta 184 (2018) 557–564.
[38] R. Rajkó, H. Abdollahi, S. Beyramysoltan, N. Omidikia, Definition and detection of data-based uniqueness in evaluating bilinear (two-way) chemical measurements, Anal. Chim. Acta 855 (2015) 21–33.
[39] S.K. Karimvand, M.A. Lakeh, E. Tavakkoli, M. Ghaffari, N. Omidikia, S.K.A. Abad, R. Rajkó, H. Abdollahi, A general rule for uniqueness in self-modeling curve resolution methods, J. Chemometr. 34 (2020) e3268.
[40] R. Rajkó, N. Omidikia, H. Abdollahi, M. Kompany-Zareh, On uniqueness of the non-negative decomposition of two- and three-component three-way data arrays, Chemometr. Intell. Lab. Syst. 160 (2017) 91–98.
[41] H. Abdollahi, R. Tauler, Uniqueness and rotation ambiguities in multivariate curve resolution methods, Chemometr. Intell. Lab. Syst. 108 (2011) 100–111.
[42] P.J. Gemperline, Computation of the range of feasible solutions in self-modeling curve resolution algorithms, Anal. Chem. 71 (1999) 5398–5404.
[43] R. Tauler, Calculation of maximum and minimum band boundaries of feasible solutions for species profiles obtained by multivariate curve resolution, J. Chemometr. 15 (2001) 627–646.
[44] R.B. Pellegrino Vidal, A.C. Olivieri, R. Tauler, Quantifying the prediction error in analytical multivariate curve resolution studies of multicomponent systems, Anal. Chem. 90 (2018) 7040–7047.
[45] J. Jaumot, R. Tauler, MCR-BANDS: a user friendly MATLAB program for the evaluation of rotation ambiguities in Multivariate Curve Resolution, Chemometr. Intell. Lab. Syst. 103 (2010) 96–107.
[46] A.C. Olivieri, R. Tauler, N-BANDS: a new algorithm for estimating the extension of feasible bands in multivariate curve resolution of multi-component systems in the presence of noise and rotational ambiguity, J. Chemometr. (2021), https://doi.org/10.1002/cem.3317 (in press).
[47] A.C. Olivieri, H.L. Wu, R.Q. Yu, MVC2: a MATLAB graphical interface toolbox for second-order multivariate calibration, Chemometr. Intell. Lab. Syst. 96 (2009) 246–251.
[48] X. Zhang, R. Tauler, Measuring and comparing the resolution performance and the extent of rotation ambiguities of some bilinear modeling methods, Chemometr. Intell. Lab. Syst. 147 (2015) 47–57.
[49] X. Zhang, Z. Zhang, R. Tauler, Evaluation of the extension of rotation ambiguity associated to multivariate curve resolution solutions by the application of the MCR-BANDS method, Talanta 202 (2019) 554–564.
[50] K. Neymeyr, A. Golshan, K. Engel, R. Tauler, M. Sawall, Does the signal contribution function attain its extrema on the boundary of the area of feasible solutions? Chemometr. Intell. Lab. Syst. 196 (2020) 103887.
[51] R.B. Pellegrino Vidal, A.C. Olivieri, A new parameter for measuring the prediction uncertainty produced by rotational ambiguity in second-order calibration with multivariate curve resolution, Anal. Chem. 92 (2020) 9118–9123.
[52] S. Bortolato, J.A. Arancibia, G.M. Escandar, Non-trilinear chromatographic time retention–fluorescence emission data coupled to chemometric algorithms for the simultaneous determination of ten polycyclic aromatic hydrocarbons in the presence of interferences, Anal. Chem. 81 (2009) 8074–8084.
[53] W. Windig, J. Guilment, Interactive self-modeling mixture analysis, Anal. Chem. 63 (1991) 1425–1432.
[54] A. Hyvärinen, J. Karhunen, E. Oja, Independent Component Analysis, John Wiley & Sons, New York, 2001.
[55] J.A. Johnson, J.H. Gray, N.T. Rodeberg, R.M. Wightman, Multivariate curve resolution for signal isolation from fast-scan cyclic voltammetric data, Anal. Chem. 89 (2017) 10547–10555.
[56] R. Manne, B.V. Grande, Resolution of two-way data from hyphenated chromatography by means of elementary matrix transformations, Chemometr. Intell. Lab. Syst. 50 (2000) 35–46.
[57] W. Windig, A. Bogomolov, S. Kucheryavkiy, Two-way data analysis: detection of purest variables, in: S. Brown, R. Tauler, B. Walczak (Eds.), Comprehensive Chemometrics, Second Edition, Chemical and Biochemical Data Analysis, vol. 2, Elsevier, Oxford, 2020, pp. 107–136 (Chapter 2).08.
[58] M.J. Culzoni, H.C. Goicoechea, G.A. Ibañez, V.A. Lozano, N.R. Marsili, A.C. Olivieri, A.P. Pagani, Second-order advantage from kinetic-spectroscopic data matrices in the presence of extreme spectral overlapping. A multivariate curve resolution - alternating least-squares approach, Anal. Chim. Acta 614 (2008) 46–57.
[59] A.C. Olivieri, G.A. Ibañez, V.A. Lozano, Second-order analyte quantitation under identical profiles in one data dimension. A dependency-adapted partial least-squares/residual bilinearization method, Anal. Chem. 82 (2010) 4510–4519.
[60] G. Ahmadi, H. Abdollahi, A systematic study on the accuracy of chemical quantitative analysis using soft modeling methods, Chemometr. Intell. Lab. Syst. 120 (2013) 59–70.
[61] M.R. Alcaraz, M.J. Culzoni, G.A. Ibañez, V.A. Lozano, A.C. Olivieri, On second-order calibration based on multivariate curve resolution in the presence of highly overlapped profiles, Anal. Chim. Acta 1096 (2020) 53–60.
[62] A.C. Olivieri, N. Omidikia, Initialization effects in two-component second-order multivariate calibration with the extended bilinear model, Anal. Chim. Acta 1125 (2020) 169–176.
[63] F. Chiappini, F. Gutierrez, H.C. Goicoechea, A.C. Olivieri, Analytical second-order advantage with first-order instrumental data and multivariate curve resolution. When and why? Anal. Chim. Acta (2021) (submitted for publication).
[64] H.C. Goicoechea, A.C. Olivieri, R. Tauler, Application of the correlation constrained multivariate curve resolution alternating least-squares method for analyte quantitation in the presence of unexpected interferences using first-order instrumental data, Analyst 135 (2010) 636–642.
[65] M. Ghaffari, A.C. Olivieri, H. Abdollahi, Strategy to obtain accurate analytical solutions in second-order multivariate calibration with curve resolution methods, Anal. Chem. 90 (2018) 9725–9733.

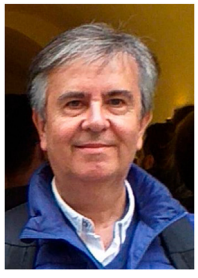

Alejandro C. Olivieri is a member of the Rosario Institute of Chemistry, and professor in the Department of Analytical Chemistry, National University of Rosario. Born in Rosario, Argentina, July 28, 1958. B.Sc. (Catholic Faculty of Chemistry and Engineering, 1982), Ph.D. (Faculty of Biochemical and Pharmaceutical Sciences, University of Rosario, 1986), fellow of the Argentinean Research Council (CONICET). About 250 publications, books and book chapters. John Simon Guggenheim Memorial Foundation fellow (2001–2002). Platinum Konex prize (Konex Foundation, Argentina, 2013) for his contributions to analytical chemistry. Current interest: chemometrics in analytical chemistry.